Preparation of poly-dopamine-silk fibroin sponge and its dye molecular adsorption

Ming Duan, Qingqing Tang, Manlin Wang, Mengjuan Luo, Shenwen Fang, Xiujun Wang, Peng Shi and Yan Xiong

ABSTRACT

This paper proposes a process for fabricating a poly-dopamine-silk fibroin sponge (PDA-SF) by using dopamine self-assembly and coating the skeleton of a silk fibroin sponge. The PDA-SF sponge was characterized by SEM, TEM, XPS, XRD and FT-IR. It was found that the sponge exhibits sheet structures with a pore size of 60 ± 20 μm and poly-dopamine adhered to the surface of pure silk fibroin through noncovalent bond forces. With a hierarchical porous structure, the derived sponge provides fast flow channels and abundant active sites, which will benefit the diffusion and removal of cationic dyes. Batch adsorption and dynamic adsorption of crystal violet (CV) were studied. The batch adsorption capacity of the PDA-SF sponge for CV increased with its PDA content. Under a dynamic adsorption mode, the adsorption efficiency of the PDA-SF sponge for CV (5 mg/L, 200 mL) can reach up to 98.2% after 12 min, whereas it is only 90.2% under stationary mode after 72 h. Furthermore, the sponge shows an outstanding smart adsorption performance. More importantly, the composite sponge still keeps high separation and adsorption efficiencies after 20 cycles, and the appearance remains good.

Key words | continuous adsorption, dye, poly-dopamine, silk fibroin

Ming Duan (corresponding author)
Qingqing Tang
Manlin Wang
Mengjuan Luo
Shenwen Fang
Peng Shi
Yan Xiong
School of Chemistry and Chemical Engineering,
Southwest Petroleum University,
Chengdu, 610500,
China
E-mail: *swpua124@126.com*

Ming Duan
Manlin Wang
Shenwen Fang
Peng Shi
Yan Xiong
Oil & Gas Applied Chemistry Key Laboratory of Sichuan Province,
Chengdu, 610500,
China

Xiujun Wang
Beijing Research Center of China National Offshore Oil Corporation,
Beijing, 100027,
China
and
State Key Laboratory of Offshore Oilfield Exploitation,
Beijing, 100027,
China

HIGHLIGHTS

- A process for fabricating a poly-dopamine-silk fibroin sponge is introduced.
- The sponge shows an outstanding adsorption performance for various dye mixtures.
- A facile fabrication process with high adsorption efficiency and recyclability.

GRAPHICAL ABSTRACT

INTRODUCTION

Water pollution is now becoming an increasingly severe issue due to rapid development of industrialization, in which 16% of industrial effluent is from dyestuff chemical wastewater. Organic dyes are universally recognized as one of the chemical dye products, which are mainly derived from the textile factories, leather, coating etc. Most of these

doi: 10.2166/wst.2020.502

chemical dyestuff products have a complex structure and high toxicity and are difficult to degrade (Asuha *et al.* 2010; Saha *et al.* 2011; Song *et al.* 2013; Rehman *et al.* 2020). If these dyestuffs were discharged into water ecosystem, human beings and even the entire ecosystem would be in danger. So far, the current methods, which include membrane filtration (Arica *et al.* 2017; Chen *et al.* 2017), electrochemical (Brillas & Martinez-Huitle 2015), biochemical (Balapure *et al.* 2016; Bayramoglu *et al.* 2017) and adsorption (Fu *et al.* 2014; Bayramoglu *et al.* 2016; Arica *et al.* 2019; Tahira *et al.* 2019) etc. are used for removing the organic dyes from water. Sponge adsorption is considered as an effective strategy because of its high adsorption capacity, recyclability and easy operation (Zhao *et al.* 2012). Wang and co-workers fabricated a PU@RGO@MnO_2 sponge for the removal of methylene blue (Wang *et al.* 2016a). The modified sponges commonly used for adsorption are polyurethane (PU) sponge (Ke *et al.* 2014; Wang *et al.* 2014; Wu *et al.* 2014), melamine sponge (Pham & Dickerson 2014) etc. But they are not biodegradable, which means there could be secondary pollution. In this way, the design of an easily fabricated and eco-friendly porous 3-D structure for water purification is still highly demanded.

Silk fibroin (SF) has become an alternative candidate for processing into various material formations (Xia & Lu 2008; Rockwood *et al.* 2011; Silva *et al.* 2012; Ling *et al.* 2016) such as sponges, hydrogels, fibers, films, and membranes due to its excellent biocompatibility, mechanical properties, and robust flexibility (Rockwood *et al.* 2011). Freeze-drying is a widely used way to fabricate silk fibroin sponges, which have a hierarchical structure with high porosities and controllable aperture sizes. However, there is limited report on dyes' adsorption with silk fibroin-based sponge, while silk fibroin-based sponge has been mainly applied in tissue engineering, drug carriers and the controlled release of drugs (Wang *et al.* 2006; Pritchard & Kaplan 2011).

Poly-dopamine (PDA) is a catechol derivative, containing numerous functional groups, such as catechol groups, amine groups and aromatic groups, which provide a large number of active binding sites for those contaminants (Liu *et al.* 2014). For example, Fu and co-workers used an oxidative polymerization method to fabricate poly-dopamine microspheres as absorbents for water treatment and showed the adsorption capacity for methylene blue at 25 °C could reach up to 90.7 mg/g (Fu *et al.* 2015). Although as a micro-structured material, poly-dopamine has excellent adsorption and removal capability for organic dyes, difficult separation from treated water is still a drawback. Dopamine (DA), also known as bio-inspired 'glue', contains abundant catechol and amine groups, and they can simulate adhesive protein. Moreover, it can be oxidized and self-polymerized into poly-dopamine, which exhibits a stable adhesive in almost all solid substrates (Wang *et al.* 2015).

In the present study, we report an approach to fabricate sponges derived from natural *Bombyx mori* silk fibroin. Firstly, pure silk fibroin sponge was fabricated via the freeze-drying method with a hierarchical porous structure and it was modified by dopamine through a simple dip-coating step to obtain PDA-SF sponge. Then, as-prepared hybrid sponges were characterized in detail. Finally, the adsorption and separation performance for various dyes were systematically investigated. Compared to poly-dopamine, monolithic PDA-SF sponge was easy to separate and reuse as a bulk absorbent, avoiding a troublesome separation process in treated water. Moreover, the hierarchical porous structure was beneficial to the diffusion of dye contaminants to improve the adsorption and removal efficiencies. Furthermore, the absorbed dyestuffs were eluted by aqueous ethanol, which not only benefited recycling but also induced silk fibroin to crystallize to form a crystalline β-sheet structure, which is the most stable conformation in the silk fibroin to enhance the mechanical robustness and stability in an aqueous environment (Xiao *et al.* 2011). This study provides a novel sponge and some useful insights for dye wastewater treatment.

EXPERIMENTAL

Materials

Silkworm cocoons of *Bombyx mori*, industrial grade, were purchased from Alibaba. LiBr, 99.99%; dopamine hydrochloride, 98.0%; tris(hydroxymethyl) aminomethane, ≥99.99%; Rhodamine B, ≥99.0%; methylene blue, ≥98.5%; crystal violet (CV), ≥90.0%; Rhodamine 6G, 95.0%; methyl orange, 95.0%; methyl blue, 99.0%; new coccine, 85.0%; metanil yellow, ≥98.0%; and ethanol, 75%, were obtained from Aladdin. $NaHCO_3$, 99.5%; sodium hydroxide, 96%; hydrochloric acid, 31.0% and dialysis tubing were supplied by Chengdu Kelong Chemical Co., Ltd.

Preparation of silk fibroin sponge

The silk fibroin solution was prepared through a degummed method (Chen *et al.* 2008). Briefly, silkworm cocoons were cut into suitable pieces to boil in an aqueous solution of 2 wt % $NaHCO_3$ for 20 mins. Later on, this procedure was

repeated once more to remove sericin. During this procedure, fibers were subsequently rinsed with deionized water several times and dried at 60 °C. Sericin-free silk fibers were dissolved in a 9.5M LiBr solution at 60 °C for 72 h, the obtained solution was dialyzed with deionized water by a dialysis tube (Pierce, MWCO 3500) for 72 h. Then, the dialyzed solution was purified through centrifugation at 5,000 rpm for 20 min. A weighing method was used to measure the concentration of the final solution, and it showed the concentration rate is about 4%. For further study, the resulting solution was then stored in a refrigerator under 2 °C. Silk fibroin solution was poured in 8-well polystyrene culture plates, which were frozen at −20 °C overnight, and then freeze-dried for 72 h. The obtained sponge was immersed in 90% (v/v) ethanol solution for 2 h and then ethanol was evaporated at 60 °C. Finally, the pure silk fibroin sponge was obtained.

Fabrication of 3D PDA-SF sponges

In this study, pure silk fibroin sponges were immersed in different concentrations of dopamine solution (25 mg/mL, 50 mg/mL, 75 mg/mL, 100 mg/mL) at pH = 8.5 to obtain PDA-SF sponges, which are labelled as 25-PDA-SF, 50-PDA-SF, 75-PDA-SF, 100-PDA-SF sponge. Poly-dopamine solutions was prepared according to an oxidative polymerization route for 72 h (Fu *et al.* 2015). Dopamine powder was dissolved in Tris buffer (10 mM pH = 8.5) solution, and magnetically stirred for 12 h at ambient temperature. The PDA-SF sponges were rinsed with deionized water several times, then dried at 60 °C.

Characterization

The surface morphology and cross-sectional morphology of the sponge were characterized by QUANTA F250 scanning electron microscope (SEM, FEI Corp., USA). The dopamine adhesion to the sponge was observed by Tecnai G2 F20 transmission electron microscope (TEM, FEI Corp., USA). The surface chemical state of the sponge was analyzed by Thermo ESCALAB 250XI X-ray electron spectroscopy (XPS, Thermo Fisher Scientific Corp., USA). The chemical structure of the sponge was determined by Thermo Fisher Nicolet 6700 FTIR spectrometer (Thermo Fisher Scientific Corp., USA). Cu Kα ray was used to determine the X-ray diffraction patterns of the sponge determined by X-ray powder diffraction (XRD, PANalytical Company, Netherlands). Ultraviolet spectrum determination was conducted on a UV-1800 spectrometer (Shimadzu Corp, Japan).

Batch adsorption

The adsorption of CV on the sponge was evaluated by batch experiments at room temperature. Each 6 g of sponge was put in CV solution (200 mL, 5 mg/L) in a beaker. 5 mL of solution was collected at regular time intervals (1–72 h) and the CV concentration was measured by UV-1800 spectrometer. The adsorption capacity (q_e) was calculated according to formula (1)

$$q_e = \frac{(C_0 - C_t)V}{W_0} \tag{1}$$

where, C_0 is the initial concentration of CV, Ct is the concentration of CV at t moment, V is the volume of CV solution and W_0 is the mass weight of sponge.

Dynamic adsorption

The crystal violet solution with an initial concentration of 5 mg/L is used for continuous dynamic adsorption experiments depending on the continuous dynamic adsorption device (as shown in Figure 1).The concentration of the crystal violet solution after absorption is also measured by the ultraviolet-visible spectrum and the adsorption efficiency of poly-dopamine-silk fibroin sponge (PDA-SF) is also calculated by equation (1).

Figure 1 | The continuous dynamic adsorption device.

RESULTS AND DISCUSSION

Morphology of the sponges

Figure 2(a) shows the surface SEM image of the SF sponge. From this picture, the SF sponge shows a surface having no obvious pore structure. Figure 2(b) and 2(c) show the fracture surface SEM images of the SF sponge. Figure 2(b) shows that the layers are placed one above the other and Figure 2(c) displays an interconnected network and porous structure with the general pore size of 60 ± 20 μm (see Figure 2(d)). This interconnected network and porous structure provide a high flux for continuous dynamic absorption of dye solution. Condensed and compact flakelike layers were also observed, making the sponge less brittle and insoluble in water (Nazarov *et al.* 2004).

Figure 2(e) is the surface SEM image of the PDA-SF sponge. From this picture, we can see that its surface is much rougher than that of SF sponge. The rough surface was caused by the poly-dopamine, which was spontaneously synthesized from dopamine under alkaline conditions via an oxidative polymerization method. Because there was zero geometrical hindrance, poly-dopamine were formed and adhered to the skeleton of silk fibroin sponge through the interactions of non-covalent bonds (Xu *et al.* 2010; Kim *et al.* 2014). Figure 2(f)–2(i) are the TEM images of a series of PDA-SF sponges that were prepared with dopamine solution at different concentrations. As it shows, the poly-dopamine microspheres were free-standing and uniformly distributed on the skeleton of the SF sponge with a diameter of 0.195 μm when the concentration of dopamine was 25 mg/mL (Figure 2(j)). However, the diameter decreased to 0.067 μm when the concentration increased to 50 mg/mL (Figure 2(k)). Furthermore, when it continued to increase to 75 mg/mL, as-synthesized poly-dopamine microspheres gradually gathered together. This means the poly-dopamine that adheres to the SF sponge may be saturated.

Structure details of the sponges

XPS was used to examine the surface atomic chemical composition of the sponges in detail. The XPS survey scans of pure silk fibroin sponge and the PDA-SF sponge are shown in Figure 3(a). As can be seen, three characteristic peaks corresponding to C1s (binding energy, 284 eV), N1s (binding energy, 399 eV), and O1s (binding energy, 532 eV) displayed similar levels in both pure SF sponge and PDA-SF sponge. However, the intensity of the PDA-SF sponge was stronger than that of pure SF sponge. Atomic ratios of carbon, nitrogen and oxygen on pure SF and the PDA-SF sponges were calculated from the XPS survey scan spectra. The content of carbon, nitrogen, and oxygen on the pure SF sponge was 78.17%, 6.52%, and 15.3%, respectively. The content of carbon, nitrogen, and oxygen on the PDA-SF sponge is 69.86%, 8.92%, and 21.22%, respectively. The PDA-SF sponge showed a slightly higher amount of N and O atoms than the pure silk fibroin with the percentage increasing by 2.40% and 5.92% respectively, indicating that the sponge surface was partly covered with the poly-dopamine, which had the same elements as the pure silk fibroin.

In high-resolution C1s spectrum of pure silk fibroin (Figure 3(b)), the peaks are composed of four different carbon atoms types: 288.2 eV (N-C = O), 286.1 eV (C-O), 285.0 eV (C-N) and 284.6 eV (C-C) (Wang *et al.* 2016b; Chen *et al.* 2017; Ko *et al.* 2018). Although the C1s spectrum of pure silk fibroin and PDA-SF sponge (Figure 3(c)) exhibited the majority of similar peaks, there was a significant increase in 285.1 eV (C-N) and in 286.2 eV (C-O), which was due to the functional groups from the poly-dopamine. The decrease in 284.5 eV (C-C) was also attributed to the coating of poly-dopamine on the surface of pure silk fibroin sponge. The high-resolution N1s and O1s spectra (Figure 3(d) and 3(e)) were also utilized to confirm the functional groups on the sponge in detail. As for the pure silk fibroin, the N1s scan spectrum was split into two peaks: 400.1 eV (N-C = O), and 399.6 eV (C-N), and in the O1s scan spectrum, three peaks were split up: 532.4 eV (C-O), 531.7 eV (N-C = O), and 531.1 eV (C = O). For the PDA-SF sponge (Figure 3(f) and 3(g)), the N1s displayed two similar deconvolution peaks with the pure SF sponge; in addition, there was an increase of 399.7 eV (N-C) as the presence of poly-dopamine layer coating on pure silk fibroin. As for the O1s spectrum, peaks centered at 533.4 eV, 532.6 eV, 531.5 eV and 530.8 eV demonstrated four types of O bounding in the sponge, and the new peak at 533.3 eV was characteristic of O-C = O, which could be corresponded to the groups originated from the poly-dopamine. All the spectra indicated that the poly-dopamine was successfully introduced and capped on the surface of pure silk fibroin silk sponge.

Crystal structure is important for the mechanical strength of the sponge and X-ray diffraction was used for investigating the crystal structures of different sponges. Figure 4 shows the X-ray diffraction patterns of different sponges. Compared with the untreated pure SF sponge,

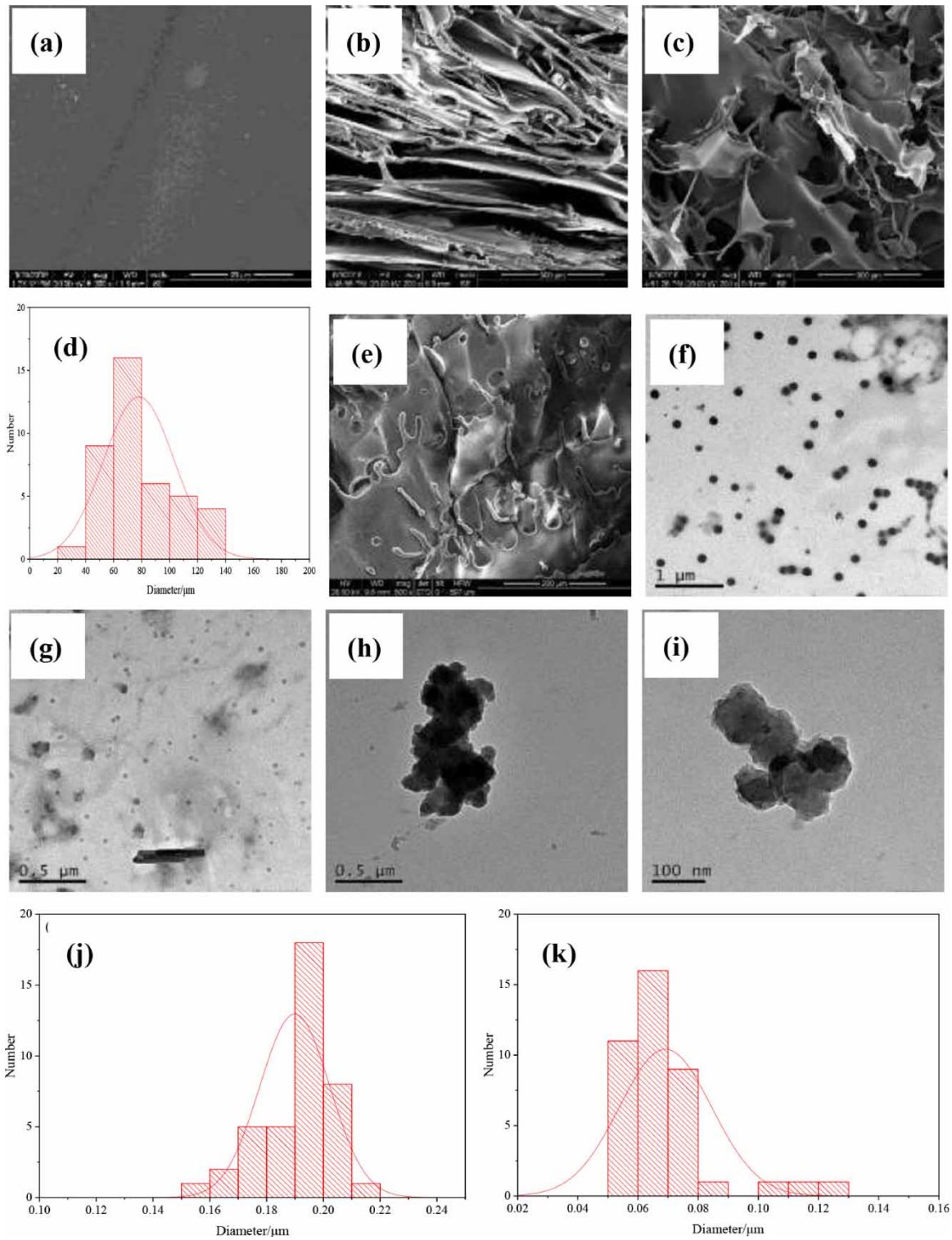

Figure 2 | The (a) surface and (b) (c) fracture surface SEM images of SF sponge; (d) pore distribution of SF sponge; (e) the surface SEM image of PDA-SF sponge; the TEM image of (f) 25-PDA-SF; (g) 50-PDA-SF; (h) 75-PDA-SF; (i) 100-PDA-SF sponge; the size distribution of poly-dopamine synthesized with the concentration of (j) 25 mg/mL; (k) 50 mg/mL dopamine.

two distinct peaks appeared at $2\theta = 20.28°$ and $2\theta = 24.41°$ are attributed to the β-sheet (silk II) crystalline structure (Kim *et al.* 2005). Silk fibroin consisted of three different forms, namely random coil, α-form (silk I) and β-form (silk II), which existed in an antiparallel β-sheet structure (Tadepalli *et al.* 2016). When the pure SF sponge was

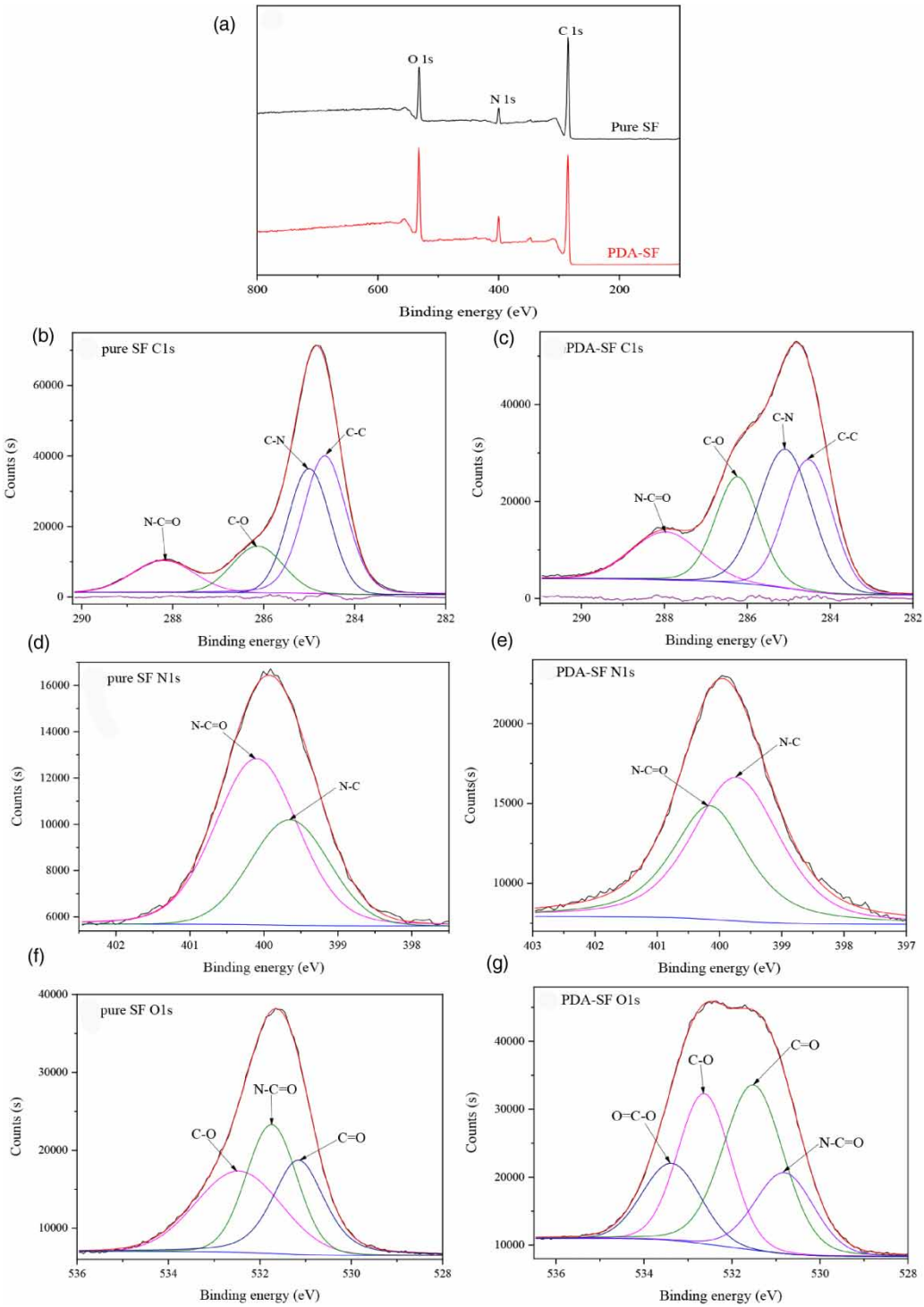

Figure 3 | (a) X-ray photoelectron spectroscopy survey scan spectra of pure silk fibroin sponge and the PDA-SF sponge; (b) C1s spectrum of pure silk fibroin sponge; (c) C1s spectrum of the PDA-SF sponge; (d) N1s spectrum of pure silk fibroin sponge; (e) N1s spectrum of the PDA-SF sponge; (f) O1s spectrum of pure silk fibroin sponge; and (g) O1s spectrum of the PDA-SF sponge.

exposed to ethanol, the ethanol enabled the dehydration of hydrated hydrophobic domains to form chain-chain contact and antiparallel β-sheet structure (Nazarov *et al.* 2004; Xiao *et al.* 2011). The β-sheet structure not only enhanced the mechanical strength of the SF sponge, but also ensured the stability of the SF sponge in aqueous

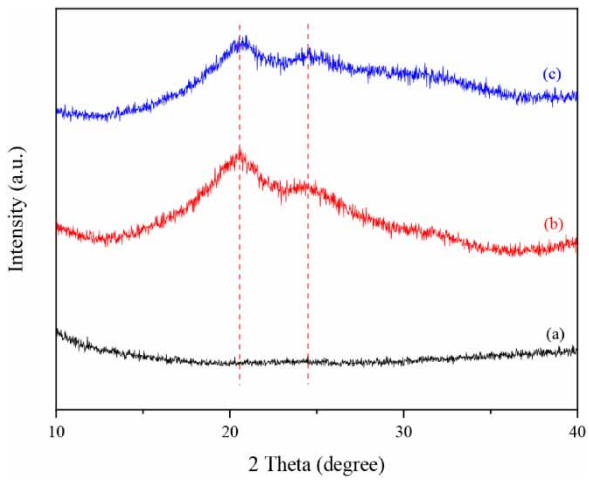

Figure 4 | X-ray diffraction patterns of (a) untreated pure SF sponge; (b) pure SF sponge treated with ethanol solution; (c) ethanol treated pure SF sponge coated by poly-dopamine.

environment. There is no significant difference between the PDA-SF sponge and ethanol-treated pure SF sponge, which suggested that the PDA coating did not affect the crystal structure of the fibroin (Lu *et al.* 2015).

Fourier transform infrared (FT-IR) spectroscopy was used to investigate the secondary structure of the sponge. The FT-IR adsorption region of 1,700 cm^{-1} to 1,500 cm^{-1}, which is assigned to the peptide backbones of Amid I (1,700 cm^{-1} to 1,600 cm^{-1}) and Amid II (1,600 cm^{-1} to 1,500 cm^{-1}), is usually used to analyze the secondary structure of protein because it is very sensitive to the secondary structures (α-helix, β-sheet, β-turn, and random coil), especially for the Amid I band (Tadepalli *et al.* 2016).

Compared to the silk fibroin sponge not treated by the ethanol solution, the peaks of treated sponge in the region of 1,700 cm^{-1} to 1,500 cm^{-1} are all enhanced, as shown in Figure 5(a). The characteristic peaks at 1,645 cm^{-1} (Amid I), 1,521 cm^{-1} (Amid II), and 1,236 cm^{-1} (Amid III), which were attributed to the random coil and β-sheet structures respectively, were observed in the spectra of pure silk fibroin sponge before it was treated by the ethanol. For the treated SF sponge, the observed characteristic peak at 1,692 cm^{-1} (Amid I) is assigned to the β-sheet structure, and the small shoulder at 1,632 cm^{-1} (Amid I) is assigned to random coil. The characteristic peaks at 1,516 cm^{-1} (Amid II), and

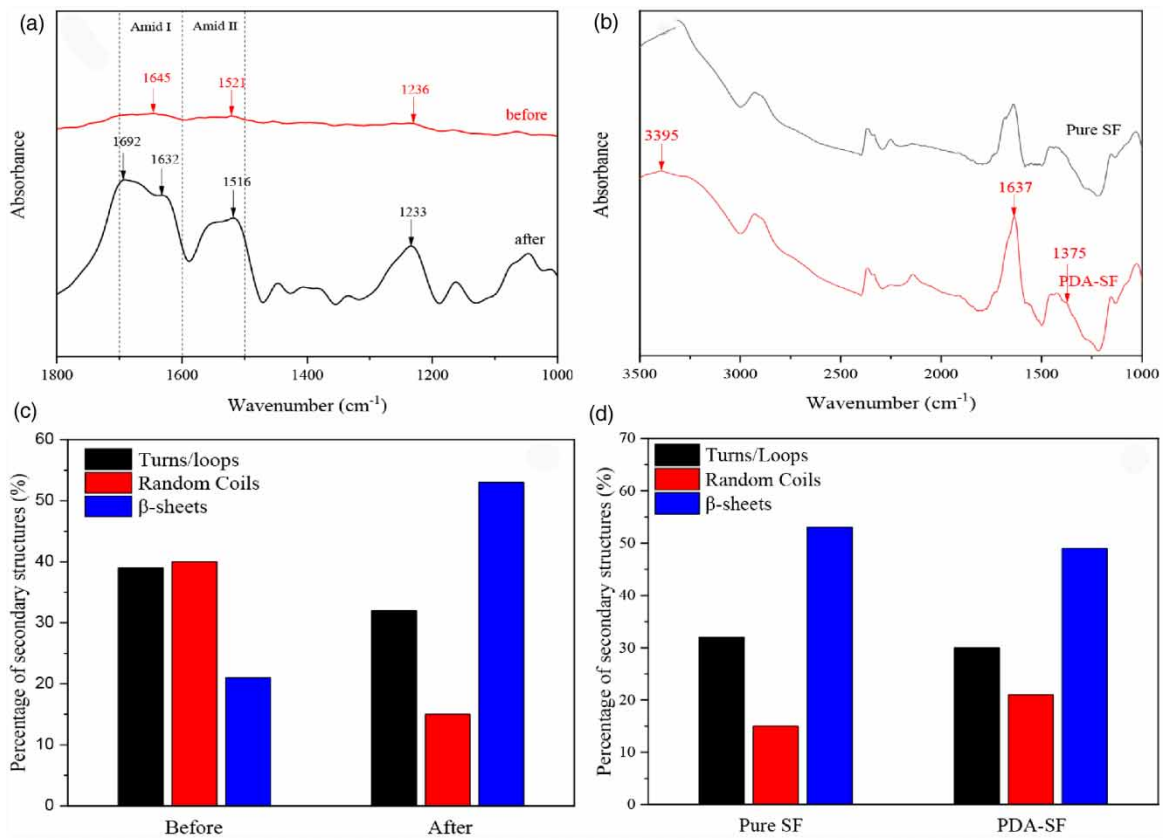

Figure 5 | FT-IR spectra of (a) SF sponge before ethanol treatment and after; (b) SF sponge and PDA-SF sponge; percentage of different conformations of silk (c) in the SF sponge before ethanol treatment and after, and (d) in the PDA-SF sponge.

1,233 cm^{-1} (Amid III) are attributed to the β-sheets of anti-parallel β-sheet structure. The result showed that the random coil and β-sheet structure existed at the same time in the ethanol-treated SF sponge; however, the β-sheet structure plays a dominant role. As for the PDA-SF sponge (see Figure 5(b)), the adsorption band at 3,395 cm^{-1} is ascribed to the stretching vibration of phenolic O-H and N-H; the peak at 1,637 cm^{-1} can be assigned to the stretching vibration of the aromatic ring and bending vibration of N-H; and the peak at 1,375 cm^{-1} can be attributed to the bending vibration of phenolic O-H. The results show that there is PDA in the PDA-SF sponge.

To further investigate the inner transformation in silk fibroin sponges in detail, the Amid I band was deconvoluted to quantitatively analyse the composition of different secondary structures. Figure 5(c) shows that the corresponding percentages of different secondary structures (turns/loops, random coils and β-sheets) obtained from the de-convoluted spectra of SF sponge before and after ethanol treatment. As is known, polar solvent can induce crystallization in silk fibroin, and the β-sheet is the most stable structure. Compared to the pure silk fibroin sponge not treated by ethanol, the content of the β-sheet structure increased from 21% to 53% in the pure silk fibroin sponge that was treated by ethanol. Furthermore, the contents of both random coil and turns/loops structures were reduced. Figure 5(d) shows the percentage of different secondary structures of 75-PDA-SF sponge. These results indicated that the poly-dopamine may adhere to the surface of pure silk fibroin through noncovalent bond forces, so it has little impact on secondary structure change of the sponge (see Figure 6). FT-IR results indicated that the β-sheets conformation played an important role in the crystalline structure of the sponge, which is helpful for the sponge exhibiting excellent mechanical strength and stability in an aqueous environment.

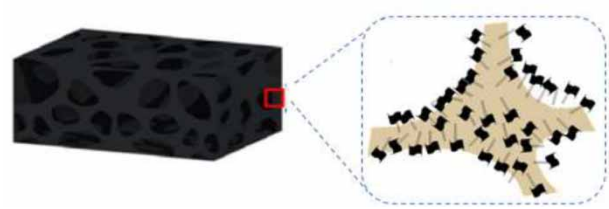

Figure 6 | The poly-dopamine adheres to the skeleton through the noncovalent bond forces.

Batch adsorption performance

Four PDA-SF sponges were used for the batch adsorption experiment. The sponges have a smaller density, and float on the aqueous solution (see Figure 7(a)). The dye molecules

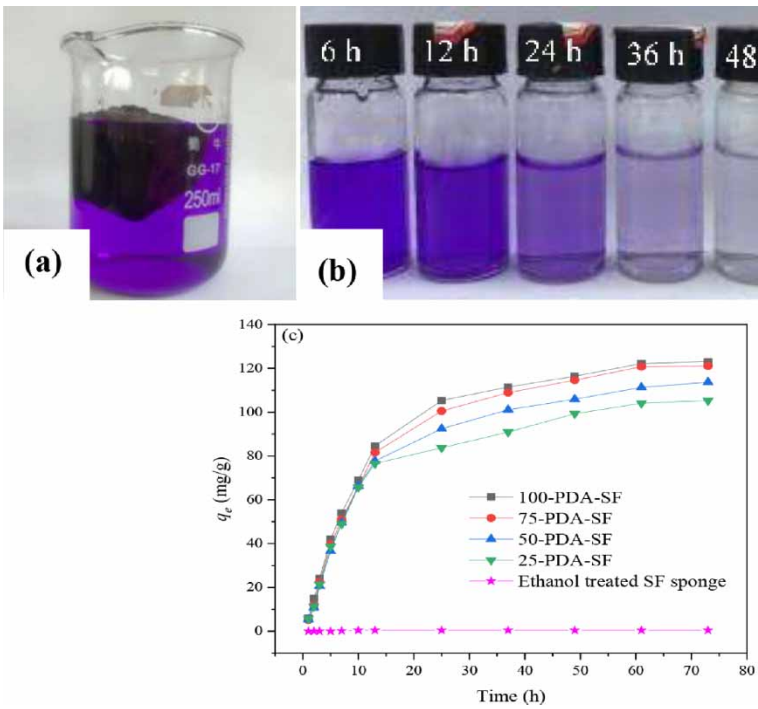

Figure 7 | (a) Photograph of 75-PDA-SF sponge floating on the aqueous CV solution; (b) the picture of CV solution absorbed by the 75-PDA-SF sponge at different times; (c) effects of contact time on the adsorption capacity of aqueous CV solution onto the PDA-SF sponges at initial concentration of 5 mg/L.

diffused onto the active sites and bonded with them via electrostatic interaction, π–π stacking interactions etc. (Fu *et al.* 2015), then the PDA-SF sponge absorbed dyes like a floating 'magnet'. Aqueous crystal violet (CV) solution with an initial concentration of 5 mg/L was utilized to do the test, the photograph of collected CV aqueous solution absorbed by 75-PDA-SF sponge at regular time intervals is presented in Figure 7(b) and the effects of contact time on four kinds of PDA-SF sponges' adsorption capacity are plotted in Figure 7(c). As can be seen, in the first 13 h, all the curves increased drastically, and showed little difference in the concentration of crystal violet that was left in the aqueous solution; then they raised gently over the remaining 59 h. In general, with the increase of dopamine concentration the as-prepared PDA-SF sponge showed a better performance at the same moment. The adsorption capacity on unit weight of materials increased with the dopamine concentration due to more poly-dopamine being synthesized and adhering to the pure silk fibroin sponge with the higher concentration of dopamine solution, and more active sites and powerful electricity being provided by the poly-dopamine for the dye contaminates. However, the advantage of 100-PDA-SF sponge is not significant, the curve is close to that of 75-PDA-SF sponge. At the concentration of dopamine of 75 mg/mL, the as-synthesized poly-dopamine attached to the skeleton of pure silk fibroin sponge might be almost saturated. Even though the concentration of dopamine was increased, the adsorption performance of 100-PDA-SF sponge was hardly improved. Furthermore, under the stationary mode, the adsorption of theses sponges depended on the movement of dye molecules in the solution.

Dynamic adsorption and separation performances

Dynamic adsorption of CV solution by 75-PDA-SF was conducted. It was found that a small piece of our 75-PDA-SF sponge (3*3*3 cm^3, 6.89 g) could be utilized to absorb aqueous CV solution continuously, at least 2 L with high adsorption efficiency (the time used by 75-PDA-SF for treating every 200 mL CV solution is about 12 min). The photographs of crystal violet solution after being continuously absorbed are presented in the inset in Figure 8 for different volumes. It was observed that the visual color of the filtrate solutions became lilac from transparent with the increase of absorbed aqueous CV solution volume. The UV-Vis spectra presented in Figure 8 further confirmed the visual observation, and the calculated absorption efficiency with respect to the different absorbed aqueous CV solution is plotted in the inset in Figure 7. It can be seen that the

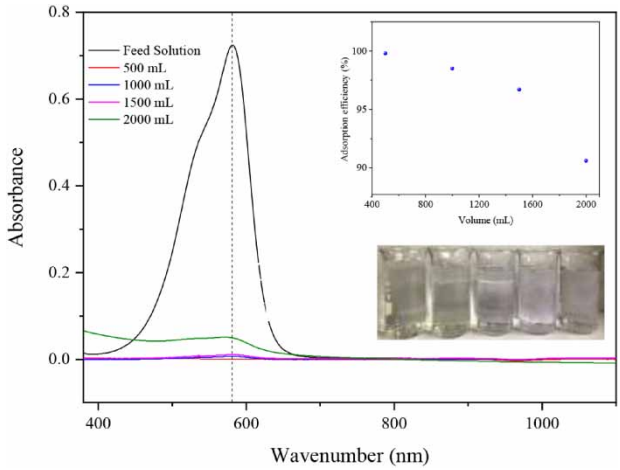

Figure 8 | The UV-Vis spectra of aqueous CV solution after being absorbed for 2 L by the 75-PDA-SF sponge (the inset is the calculated adsorption efficiency with respect to the different aqueous CV solution volumes, and the respective photographs).

adsorption efficiency was up to 98.2% for the first 100 mL, then declined to 90.6% after absorbing 2,000 mL aqueous CV solution with an initial concentration of 5 mg/L. As was discussed above, the inner structure of SF sponge is a multilayer 3D structure with general pore sizes of 60 ± 20 μm, and the poly-dopamine adhering to the skeleton of SF sponge is also in a sheet structure. The dye was absorbed by the sponge, resulting in transparent, clean water in the Buchner flask.

The dynamic adsorption performance of 75-PDA-SF sponge was studied for continuous adsorption of 200 mL of different dye solutions with an initial concentration of 5 mg/L. The results are listed in Table 1. As for other positively charged dyes; for instance, methylene blue, the adsorption efficiency reached a high percentage, to 98.6%, while for negatively charged dyes, the PDA-SF sponges showed poor performance. The reason is that the poly-dopamine synthesized under alkaline conditions was negatively charged (Fu *et al.* 2015), hence the positively charged dyes could be absorbed by the PDA-SF sponges through electrostatic interaction. Although Rhodamine B is also a cationic dye, the PDA-SF sponge showed a relatively lower adsorption capacity. The reason may be the existence of long alkyl chains causing space steric hindrance, which weakens the electrostatic interaction, and π-π stacking interaction (Fu *et al.* 2016; Zahir *et al.* 2020).

It was found that the adsorption efficiency of negatively charged dyes would change with the pH of the dye solution. The concentration of feed solution and filtrated new coccine (NC) and methyl orange (MO) at different pH were

Table 1 | Dynamic adsorption performance of 75-PDA-SF sponge for various dye molecules

Name	Formula	M_w (g mol^{-1})	pH	Analyte charge	Adsorption efficiency (%)
Crystal violet	$C_{25}H_{48}N_3Cl$	407.98		+	98.2
Methylene blue	$C_{16}H_{18}N_3SCl$	319.85		+	98.6
Rhodamine B	$C_{28}H_{31}ClN_2O_3$	479.01		+	84.8
Rhodamine 6G	$C_{28}H_3ON_2O_3$	442.55		+	88.6
New coccine	$C_{20}H_{11}N_2Na_3O_{10}S$	604.47	7.3	−	46.1
New coccine	$C_{20}H_{11}N_2Na_3O_{10}S$	604.47	1.5	−	80.1
Methyl orange	$C_{14}H_{14}N_3SO_3Na$	327.33	6.7	−	36.8
Methyl orange	$C_{14}H_{14}N_3SO_3Na$	327.33	1.5	−	88.1
Metanil yellow	$C_{18}H_{14}N_3NaO_3S$	375.38	7.2	−	23.8
Metanil yellow	$C_{18}H_{14}N_3NaO_3S$	375.38	1.5	−	92.4
Methyl blue	$C_{37}H_{27}N_3Na_2O_9S_3$	799.80	7.1	−	28.4
Methyl blue	$C_{37}H_{27}N_3Na_2O_9S_3$	799.80	1.52		90.7

monitored by the UV-Vis spectra. The concentration of filtrated solution of both NC and MO had a sharp decease to lower values when they were in acid situations, while the adsorption efficiency increased from 46.1% to 80.1% and 31.8% to 88.1% (as seen in Table 1), respectively. This result might be caused by the charge of PDA, which would change with the different solution pH (Fu *et al.* 2016); when PDA was exposed to an acid condition, the amino group on poly-dopamine could be protonated with H^+ in the solution, so they would be positively charged. Figure 9 shows the charge of poly-dopamine at different pH, (Rehman *et al.* 2020); the equipotential of poly-dopamine is about 3. When the pH value of the solution ranges from 3.5 to 10.5, the poly-dopamine is negatively charged; however, when the pH value is lower than 3, the surface zeta potential of poly-dopamine becomes positive.

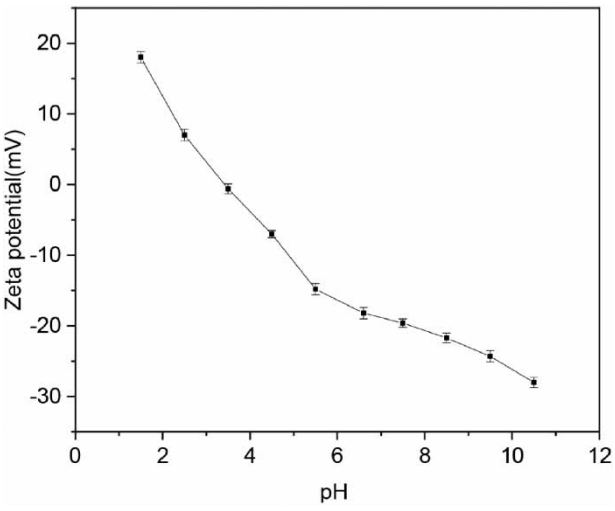

Figure 9 | Zeta potential of poly-dopamine at different pH.

Moreover, the results provided us with a clue that the PDA-SF sponge might have further applications in smart selective adsorption of dye mixtures. Generally, when an aqueous solution of dye mixture passed through the PDA-SF sponge, only positively charged dyes would be removed from the aqueous solution, while the negatively charged dyes would remain. The smart selective separation performance of the PDA-SF sponges was evaluated by absorbing the mixture solution of NC/CV, MO/CV, MB/MO and MO/Rh B, at initial concentrations of 5 mg/L. UV-Vis spectra were used to monitor the concentrations of the dyes in feed solution and the filtrate. As shown in Figure 10, the concentration of positively charged dyes diminished drastically after adsorption, while the negatively charged dyes hardly decreased and remained in the solution. The selective separation efficiencies, calculated according to Equation (3) for NC/CV, MO/CV, MB/MO, MO/Rh B, was 96.80%, 98.23%, 98.60%, 95.02% respectively.

Recycle experiments

Recyclability is also an important factor to evaluate the adsorption performance of an adsorbent. The dyes adsorbed on sponges were washed away by ethanol. On the one hand, the ethanol would facilitate the structure of silk fibroin to β-sheet structures, which would improve the mechanical property of the PDA-SF sponge to make the sponge more stable in aqueous solution; on the other hand, the dyes and ethanol could be recovered by rotary evaporation.

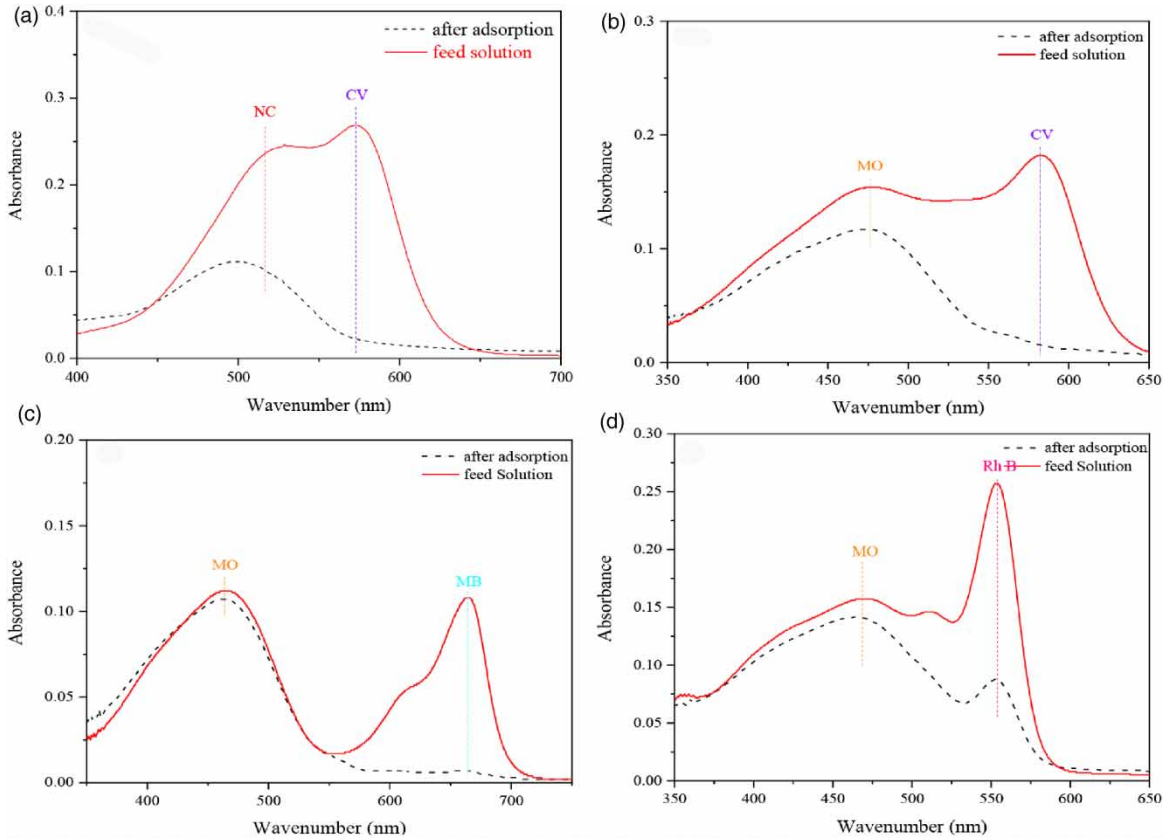

Figure 10 | UV-Vis spectra of mixed dye solutions before and after adsorption. (a) new coccine/ crystal violet; (b) methyl orange/crystal violet; (c) methyl orange/ methylene blue; (d) methyl orange/Rhodamine B.

75-PDA-SF sponge was washed by ethanol and deionized water 3 times each, dried at 65 °C, and then was used to perform adsorption tests on crystal violet/methyl orange mixed solution, and the whole process was repeated 20 times. Results of each selective separation efficiency was illustrated in Figure 11. the adsorption efficiency has slumped from 98.50% to 95.72%, only declined by 2.8%, and the sponge still obtains.

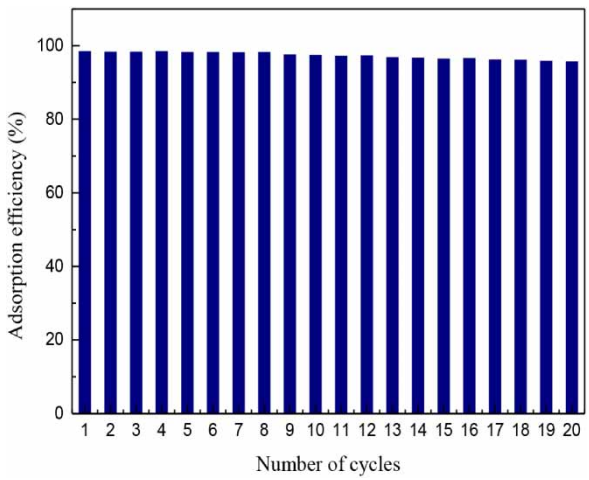

Figure 11 | Recyclability of the 75-PDA-SF sponge in smart adsorption of crystal violet/ methyl orange mixed solution.

CONCLUSION

In conclusion, this paper researched the fabrication of novel PDA-SF sponge by self-assembling of dopamine on the skeleton of pure silk fibroin sponge, which was derived from natural *Bombyx mori* silk. The pure silk fibroin sponge, fabricated by the freeze-drying method, has a multilayer 3D structure with pore size of 60 ± 20 μm, which guarantees the sponge is less brittle and insoluble in water and has a high flux level. Antiparallel β-sheet conformation dominates the crystalline structure of the sponge due to the interaction of ethanol and fibroin. It endows the sponge with enhanced robustness and stability in an aqueous condition. Negatively charged poly-dopamine was self-polymerized by dopamine under alkaline condition and adhered to the

surface of pure silk fibroin sponge through noncovalent bonding. By combining with the vacuum system, the monolithic porous sponge performed as a filter and generated an outstanding ability for smart adsorption of various dye mixtures. Furthermore, ethanol can elute the dye molecules absorbed by the PDA-SF sponge for recycling; on the other hand, it facilitated the conformation of β-sheet structures, which made the sponge more robust and stable in the aqueous environment. The talented removal efficiency and recyclability make the PDA-SF sponge promising for efficient water treatment.

CONFLICTS OF INTEREST

The authors declare no conflict of interest.

ACKNOWLEDGEMENTS

The authors gratefully acknowledge the financial support offered by the National Natural Science Foundation of China (Nos. 21607174 and 51974267).

DATA AVAILABILITY STATEMENT

All relevant data are included in the paper or its Supplementary Information.

REFERENCES

Arica, T. A., Ayas, E. & Arica, M. Y. 2017 Magnetic MCM-41 silica particles grafted with poly(glycidylmethacrylate) brush: modification and application for removal of direct dyes. *Microporous and Mesoporous Materials* **243**, 164–175.

Arica, T. A., Kuman, M., Gercel, O. & Ayas, E. 2019 Poly(dopamine) grafted bio-silica composite with tetraethylenepentamine ligands for enhanced adsorption of pollutants. *Chemical Engineering Research & Design* **141**, 317–327.

Asuha, S., Zhou, X. G. & Zhao, S. 2010 Adsorption of methyl orange and Cr(VI) on mesoporous TiO_2 prepared by hydrothermal method. *Journal of Hazardous Materials* **181** (1–3), 204–210.

Balapure, K., Jain, K., Bhatt, N. & Madamwar, D. 2016 Exploring bioremediation strategies to enhance the mineralization of textile industrial wastewater through sequential anaerobic-microaerophilic process. *International Biodeterioration & Biodegradation* **106**, 97–105.

Bayramoglu, G., Arica, M. Y., Liman, G., Celikbicak, O. & Salih, B. 2016 Removal of bisphenol A from aqueous medium using molecularly surface imprinted microbeads. *Chemosphere* **150** (May), 275–284.

Bayramoglu, G., Ozalp, V. C. & Arica, M. Y. 2017 Removal of disperse Red 60 dye from aqueous solution using free and composite fungal biomass of *Lentinus concinnus*. *Water Science and Technology* **75** (2), 366–377.

Brillas, E. & Martinez-Huitle, C. A. 2015 Decontamination of wastewaters containing synthetic organic dyes by electrochemical methods. An updated review. *Applied Catalysis B-Environmental* **166**, 603–643.

Chen, X., Qi, Y. Y., Wang, L. L., Yin, Z., Yin, G. L., Zou, X. H. & Ouyang, H. W. 2008 Ligament regeneration using a knitted silk scaffold combined with collagen matrix. *Biomaterials* **29** (27), 3683–3692.

Chen, T., Duan, M., Shi, P. & Fang, S. 2017 Ultrathin nanoporous membranes derived from protein-based nanospheres for high-performance smart molecular filtration. *Journal of Materials Chemistry A* **5** (38), 20208–20216.

Fu, J. W., Chen, Z. H., Wang, M. H., Liu, S. J., Zhang, J. H., Zhang, J. N., Han, R. P. & Xu, Q. 2015 Adsorption of methylene blue by a high-efficiency adsorbent (polydopamine microspheres): kinetics, isotherm, thermodynamics and mechanism analysis. *Chemical Engineering Journal* **259**, 53–61.

Fu, J. W., Xin, Q. Q., Wu, X. C., Chen, Z. H., Yan, Y., Liu, S. J., Wang, M. H. & Xu, Q. 2016 Selective adsorption and separation of organic dyes from aqueous solution on polydopamine microspheres. *Journal of Colloid and Interface Science* **461**, 292–304.

Ke, Q. P., Jin, Y. X., Jiang, P. & Yu, J. 2014 Oil/water separation performances of superhydrophobic and superoleophilic sponges. *Langmuir* **30** (44), 13137–13142.

Kim, U.-J., Park, J., Kim, H. J., Wada, M. & Kaplan, D. L. 2005 Three-dimensional aqueous-derived biomaterial scaffolds from silk fibroin. *Biomaterials* **26** (15), 2775–2785.

Kim, J. H., Lee, M. & Park, C. B. 2014 Polydopamine as a biomimetic electron gate for artificial photosynthesis. *Angewandte Chemie-International Edition* **53** (25), 6364–6368.

Ko, E., Lee, J. S., Kim, H., Yang, S. Y., Yang, D., Yang, K., Lee, J., Shin, J., Yang, H. S., Ryu, W. & Cho, S. W. 2018 Electrospun silk fibroin nanofibrous scaffolds with two-stage hydroxyapatite functionalization for enhancing the osteogenic differentiation of human adipose-derived mesenchymal stem cells. *ACS Applied Materials & Interfaces* **10** (9), 7614–7625.

Ling, S. J., Jin, K., Kaplan, D. L. & Buehler, M. J. 2016 Ultrathin free-standing *Bombyx mori* silk nanofibril membranes. *Nano Letters* **16** (6), 3795–3800.

Liu, Y. L., Ai, K. L. & Lu, L. H. 2014 Polydopamine and its derivative materials: synthesis and promising applications in energy, environmental, and biomedical fields. *Chemical Reviews* **114** (9), 5057–5115.

Lu, Z. S., Xiao, J., Wang, Y. & Meng, M. 2015 In situ synthesis of silver nanoparticles uniformly distributed on polydopamine-coated silk fibers for antibacterial application. *Journal of Colloid and Interface Science* **452**, 8–14.

Nazarov, R., Jin, H.-J. & Kaplan, D. L. 2004 Porous 3-D scaffolds from regenerated silk fibroin. *Biomacromolecules* **5** (3), 718–726.

Pham, V. H. & Dickerson, J. H. 2014 Superhydrophobic silanized melamine sponges as high efficiency oil absorbent materials. *ACS Applied Materials & Interfaces* **6** (16), 14181–8.

Pritchard, E. M. & Kaplan, D. L. 2011 Silk fibroin biomaterials for controlled release drug delivery. *Expert Opinion on Drug Delivery* **8** (6), 797–811.

Rehman, M. Z. U., Aslam, Z., Shawabkeh, R. A., Hussein, I. A. & Mahmood, N. 2020 Concurrent adsorption of cationic and anionic dyes from environmental water on amine functionalized carbon. *Water Science and Technology* **81** (3), 466–478.

Rockwood, D. N., Preda, R. C., Yucel, T., Wang, X. Q., Lovett, M. L. & Kaplan, D. L. 2011 Materials fabrication from *Bombyx mori* silk fibroin. *Nature Protocols* **6** (10), 1612–1631.

Saha, B., Das, S., Saikia, J. & Das, G. 2011 Preferential and enhanced adsorption of different dyes on iron oxide nanoparticles: a comparative study. *Journal of Physical Chemistry C* **115** (16), 8024–8033.

Silva, S. S., Santos, T. C., Cerqueira, M. T., Marques, A. P., Reys, L. L., Silva, T. H., Caridade, S. G., Mano, J. F. & Reis, R. L. 2012 The use of ionic liquids in the processing of chitosan/silk hydrogels for biomedical applications. *Green Chemistry* **14** (5), 1463–1470.

Song, L. X., Yang, Z. K., Teng, Y., Xia, J. & Du, P. 2013 Nickel oxide nanoflowers: formation, structure, magnetic property and adsorptive performance towards organic dyes and heavy metal ions. *Journal of Materials Chemistry A* **1** (31), 8731–8736.

Tadepalli, S., Hamper, H., Park, S. H., Cao, S., Naik, R. R. & Singamaneni, S. 2016 Adsorption behavior of silk fibroin on amphiphilic graphene oxide. *ACS Biomaterials Science & Engineering* **2** (7), 1084–1092.

Tahira, I., Aslam, Z., Abbas, A., Monim-ul-Mehboob, M., Ali, S. & Asghar, A. 2019 Adsorptive removal of acidic dye onto grafted chitosan: a plausible grafting and adsorption mechanism. *International Journal of Biological Macromolecules* **136**, 1209–1218.

Wang, Y., Kim, H.-J., Vunjak-Novakovic, G. & Kaplan, D. L. 2006 Stem cell-based tissue engineering with silk biomaterials. *Biomaterials* **27** (36), 6064–6082.

Wang, Q. Q., Wang, H. H., Xiong, S., Chen, R. Z. & Wang, Y. 2014 Extremely efficient and recyclable absorbents for oily pollutants enabled by ultrathin-layered functionalization. *ACS Applied Materials & Interfaces* **6** (21), 18816–18823.

Wang, Z. X., Lau, C. H., Zhang, N. Q., Bai, Y. P. & Shao, L. 2015 Mussel-inspired tailoring of membrane wettability for harsh water treatment. *Journal of Materials Chemistry A* **3** (6), 2650–2657.

Wang, N., Li, X. F., Yang, J., Shen, Y. X., Qu, J., Hong, S. & Yu, Z. Z. 2016a Fabrication of a compressible PU@RGO@MnO_2 hybrid sponge for efficient removal of methylene blue with an excellent recyclability. *RSC Advances* **6** (91), 88897–88903.

Wang, X., Gu, Z. P., Jiang, B., Li, L. & Yu, X. X. 2016b Surface modification of strontium-doped porous bioactive ceramic scaffolds *via* poly(DOPA) coating and immobilizing silk fibroin for excellent angiogenic and osteogenic properties. *Biomaterials Science* **4** (4), 678–688.

Wu, D. X., Yu, Z. Y., Wu, W. J., Fang, L. L. & Zhu, H. T. 2014 Continuous oil-water separation with surface modified sponge for cleanup of oil spills. *RSC Advances* **4** (96), 53514–9.

Xia, Y. Y. & Lu, Y. 2008 Fabrication and properties of conductive conjugated polymers/silk fibroin composite fibers. *Composites Science and Technology* **68** (6), 1471–1479.

Xiao, W. Q., He, J. K., Nichol, J. W., Wang, L. Y., Hutson, C. B., Wang, B., Du, Y. A., Fan, H. S. & Khademhosseini, A. 2011 Synthesis and characterization of photocrosslinkable gelatin and silk fibroin interpenetrating polymer network hydrogels. *Acta Biomaterialia* **7** (6), 2384–2393.

Xu, L. Q., Yang, W. J., Neoh, K. G., Kang, E. T. & Fu, G. D. 2010 Dopamine-induced reduction and functionalization of graphene oxide nanosheets. *Macromolecules* **43** (20), 8336–8339.

Zahir, A., Aslam, Z., Aslam, U., Abdullah, A., Ali, R. & Bello, M. M. 2020 *Paspalum notatum* grass-waste-based adsorbent for rhodamine B removal from polluted water. *Chemical and Biochemical Engineering Quarterly* **34** (2), 93–104.

Zhao, J. P., Ren, W. C. & Cheng, H. M. 2012 Graphene sponge for efficient and repeatable adsorption and desorption of water contaminations. *Journal of Materials Chemistry* **22** (38), 20197–20202.

First received 15 August 2020; accepted in revised form 6 October 2020. Available online 20 October 2020